Initial oxidation of the Al(001) surface: Self-consistent electronic structure of clean Al(001) and Al(001)-$p(1\times1)$O

H. Krakauer* and M. Posternak†
Department of Physics and Astronomy, Northwestern University, Evanston, Illinois 60201

A. J. Freeman
Department of Physics and Astronomy, Northwestern University, Evanston, Illinois 60201 and Argonne National Laboratory, Argonne, Illinois 60439

D. D. Koelling
Argonne National Laboratory, Argonne, Illinois 60439
(Received 22 September 1980)

Changes due to the initial oxidation of Al(001) were determined from results of the first self-consistent thin-film calculations for the clean Al(001) surface as well as Al(001)-$p(1\times1)$O. For clean Al(001), surface state-surface resonance bands obtained for a nine-layer slab were found to be in good agreement with photoemission measurements and our earlier non-self-consistent results; its work function (4.7 ± 0.1 eV) is in good agreement with the Grepstad *et al.* experimental value (4.41 ± 0.03 eV); no surface core-level shift was found in agreement with a recent photoemission measurement; finally, the absence of an increased broadening in the surface Al($2p$) core level is discussed. For the nine-layer Al(001) plus O slab, the calculated reduction in the work function (0.6 eV) is in good agreement with the experimentally determined reduction (0.5–0.8 eV). Prominent O($2p$) peaks in the surface layer density of states at -8.0 and -10.0 eV below E_F are in good agreement with photoemission measurements. Structure at 1.0 and 1.8 eV above E_F, due to O-induced surface resonance states, are related to interface states observed by surface soft-x-ray absorption spectroscopy. The overall bonding is found to be ionic in character with charge transfer onto the O atoms. A surface core-level shift of 1.5 eV to greater binding energy is found for the surface Al atom, in excellent agreement with the Eberhardt and Kunz 1.4-eV Al($2p$) shift. It is concluded that in the initial stages of oxidation a substantial number of O atoms are chemisorbed into coplanar, fourfold hollow sites, which is consistent with a recent extended-appearance-potential-fine-structure measurement for the Al–O bond length and an earlier self-consistent cluster calculation.

I. INTRODUCTION

A fundamental understanding of the process of metallic oxidation remains as one of the basic problems in surface chemistry and physics, one which has wide-reaching consequences of great technological importance. Over the last few years, evidence has accumulated which indicates, not surprisingly, that the complex process of oxidation may proceed through stages which are conceptually quite distinct. In particular, the initial oxidation stage (perhaps involving chemisorbed overlayers of oxygen) has been extensively studied experimentally, usually on well characterized single-crystal surfaces. One of the most notable examples, which has been the subject of intense experimental investigation[1-14] is the study of the initial oxidation of Al surfaces.

Recent work on well characterized single-crystal surfaces has shown that there are basic differences in oxygen chemisorption on the low index faces of Al. While the (111) surface seems to be the best characterized face, less is known about oxide formation on the (100) and (110) faces. Based on Auger electron spectroscopy (AES) and work-function measurements, Gartland[1] proposed that thin (~5 Å) islands of Al_2O_3-like oxide form on the (100) face. While the work function changes only slightly (~0.1 eV) with oxygen exposure on the (111) and (110) surfaces, the work function decreases almost linearly[1,2] with coverage on the Al(100) surface to a saturation differences of 0.5–0.8 eV.[1] This behavior was suggested by Gartland to correlate with an island growth mechanism for this surface. Oxygen absorbed *outside* the surface, however, would be expected to cause an *increase* in work function as a result of its high electronegativity. Thus, the large decrease of the work function on the (100) surface has been taken as evidence for *incorporation* of oxygen atoms on the (100) surface—the most likely site being the fourfold hollow position. The oxidation of the (100) surface may then proceed by filling the fourfold sites together with the formation of Al_2O_3 islands.[8] A recent surface extended-appearance-potential-fine-structure[12] (EXAPFS) study also suggests the filling of the fourfold hollow site, since the Al–O spacing for ~1.5 monolayer coverage is found to be 1.98 ± 0.05 Å, which is consistent with a bond length of 2.02 Å for the fourfold site.

Photoemission studies[3-11] of the valence and core regions have also revealed qualitative differences between the three low-index faces of Al on

exposure to oxygen. Substrate core chemical shifts upon chemisorption of oxygen on Al have been observed[3,6,7] on all three faces, and there are significant differences between the different faces. The (111) surface is characterized by the appearance of two chemically shifted oxygen-derived Al $2p$ core-level peaks at greater binding energies. Below 100 L on the (111) face, a peak first appears at 1.4 eV towards greater binding energies, which is interpreted as an ordered chemisorption phase which acts as a precursor stage for oxidation.[6] At higher exposures a peak at 2.7 eV greater binding energy begins to grow, indicating the formation of the bulklike Al_2O_3 phase.[13] Low-energy-electron diffraction (LEED) measurements[6] also support the formation of a (1×1) chemisorbed phase at low coverages on the (111) face as does a recent surface EXAFS study of this surface.[12] These two chemically shifted peaks have also been observed on the (100) and (110) faces,[7] with the difference that both peaks seem to be present with nearly the same relative intensities at low coverages. Eberhard and Kunz[7] concluded that, taken together with the work-function decrease, the existence of the 1.4-eV peak on the Al(001) surface is consistent with O atoms having penetrated into the bulk. As noted above, EXAPFS studies support this conclusion.[12]

More recently, surface soft-x-ray absorption (SSXA) spectroscopy has been reported for the three low-order faces.[9,14] Using an interatomic Auger transition Al($2p$)-O($2s$), evidence for an oxygen chemisorption phase below 50 L and the existence of unoccupied interface states on these surfaces were presented.

A few theoretical calculations have been carried out for Al surfaces exposed to oxygen. Lang and Williams[15] performed self-consistent jellium calculations for an isolated O atom absorbed onto a jellium substrate. Messmer and Salahub[16] reported self-consistent cluster calculations designed to model possible surface site configurations for the adsorbed oxygen atoms, and concluded that the coplanar fourfold hollow site was the most likely. Harris and Painter[16] performed a non-self-consistent (SC) calculation for a similar but smaller cluster. Non-self-consistent slab or thin-film calculations have been performed for the (001) surface by Painter[17] and by Batra and Ciraci.[18]

In this paper, we present the first self-consistent calculation for an ordered (1×1) oxygen monolayer on the Al(001) surface in order to study the initial oxidation of this surface. In order to assess changes, we first study a clean nine-layer Al(001) slab and then the same slab with a (1×1) monolayer of oxygen atoms on each surface located in the fourfold hollow sites, i.e., coplanar with the surface Al atoms. Results for the charge density, work-function changes, surface states, and surface core-level shifts are presented which support the chemisorption of O into the fourfold sites during the initial oxidation of Al(001).

The paper is organized as follows: Sec. II briefly outlines the self-consistent film linearized augmented-plane-wave (LAPW) method of calculation; Sec. III presents our results for the clean Al(001) surface; Sec. IV presents our results for Al(001)/O and compares then to the available experimental data, and Sec. V discusses our principal conclusions.

II. METHOD OF CALCULATION

The film band-structure calculations were performed using our recently developed self-consistent film LAPW method.[19,20] As details of the self-consistent method were described elsewhere,[20] we briefly describe only those aspects specific to the present study.

In the film LAPW method, all space is partitioned into three regions: (1) touching muffin-tin (MT) spheres centered on each atomic nucleus, (2) the interstitial region between the MT spheres and (3) the vacuum region. In the present calculations, the full potential is treated in the interstitial and vacuum regions and is taken to be spherically symmetric inside the MT spheres. In bulk calculations, the use of spherically averaged potentials inside of the MT spheres and the full potential in the interstitial regions is known as the warped muffin-tin approximation[21] and appears to be an excellent approximation for metals.

The calculations were performed for a nine-layer Al(001) film and then with a (1×1) monolayer of oxygen atoms located in the fourfold hollow sites of each surface, i.e., the oxygen nuclei lie in the same plane as the Al nuclei in the surface layer. The MT sphere radius of the Al atoms in the central, $S-3$ (surface layer minus 3), and $S-2$ layer was set equal to the bulk Al touching sphere radius (2.692 a.u.). The MT radius of the Al atoms in the surface and $S-1$ layers was set equal to 2.30 a.u., and the oxygen MT radius was set equal to 1.517 a.u.

In local density-functional theory,[22] the total potential is expressed as a sum of the Coulomb and exchange-correlation potentials, $V(\vec{r})=V_{\mathrm{Coul}}(\vec{r})+V_{xc}(\vec{r})$. In this calculation, V_{xc} was set equal to the Kohn, Sham, and Gaspar[22] (KSG) $\alpha=\frac{2}{3}$ exchange potential unless otherwise indicated.

The starting potential was constructed from a superposition of overlapping spherical atomic

charge densities. Inside the MT spheres, all relativistic effects, except spin-orbit, were included[19,20,23] for the valence electrons. In each iteration, the core charge density [$(1s^2 2s^2 2p^6)$ for the Al atoms and $(1s^2)$ for the O atoms] is recomputed using the film muffin-tin potentials in a fully relativistic (i.e., including spin-orbit) Dirac-Slater-type atomic-structure program. [We note that the oxygen ($2s$) core level, treated as a valence state, has an overall dispersion of about 1.1 eV.] In the initial iterations, eigenvalues and eigenvectors are calculated at three special points[24] in the irreducible $\frac{1}{8}$ of the two-dimensional (square) Brillouin zone. In the final iterations, a ten-point set of special points[24] is used, and in the last iteration a uniform 15-k-point set is used. The symmetrized (for z reflection) basis size of, at most, 210 LAPW's yields eigenvalues which are converged to better than about 3 mRy. From the total charge density, $\rho_{\text{total}} = \rho_{\text{valence}} + \rho_{\text{core}}$, a new film potential is generated. The new potential is mixed with the current input potential to obtain the input potential for the next iteration (the largest mixing was 10% of the new potential). We considered self-consistency achieved when the maximum difference between the input potential and the output potential was less than about 0.2 eV. The eigenvalues were converged to better than 3 mRy (0.04 eV) well before the potential was converged.

III. RESULTS FOR THE CLEAN Al(001) SURFACE

As a natural starting point, we first present self-consistent results for the clean nine-layer Al(001) film.

A. Charge density and work function

As the charge density, $\rho(\vec{r})$, is the fundamental quantity in local density-functional theory, we first present the total valence charge density for the clean nine-layer Al slab in Fig. 1. The solid black circles locate the position of the Al atoms and block out the chemically uninteresting core-electron region. The nonspherical components of $\rho(\vec{r})$ inside the muffin-tin spheres were constructed using the angular momentum representation of the LAPW wave functions [Eq. (3) in Ref. 19]. The unretouched charge density in Fig. 1 exhibits minimal discontinuities across the muffin-tin sphere boundaries, which shows that satisfactory l convergence has been obtained. The bonding characteristics of the inner layers of the slab are typically metallic with a fairly constant charge density between the atoms (the average charge density is three electrons per bulk unit cell) with slight directional bonding along the body diagonals. The influence of the surface is seen to be rapidly screened out on going into the bulk, indicating

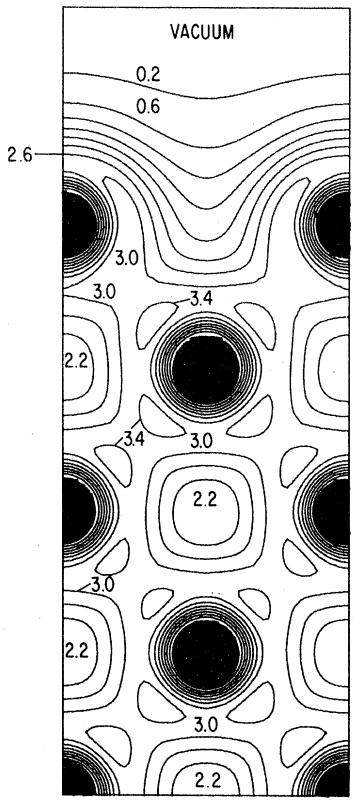

FIG. 1. Contour plot of the self-consistent total valence charge density for the upper half of the clean nine-layer Al(001) slab. Successive contours differ by 0.4 in units of electrons per bulk Al unit cell.

the ability of slab calculations to treat both bulk and surface properties. There are substantial differences, however, in the surface layer. Unlike the bulk, there is a rapid variation in $\rho(\vec{r})$ in the surface interstitial region, with $\rho(\vec{r})$ decreasing in magnitude towards the vacuum. Proceeding outward into the vacuum from the surface, $\rho(\vec{r})$ falls off sharply and soon "heals" the discrete atomic nature of the surface, i.e., $\rho(\vec{r})$ becomes nearly constant with respect to translation parallel to the surface. This sizable redistribution of charge near the surface is, of course, associated with the formation of the surface dipole layer, which sensitively determines the work function. Since the calculation for the oxygen-covered surface employed the KSG ($\alpha = \frac{2}{3}$) exchange correlation potential, $V_{\text{xc}}^{\text{KSG}}$, we also used $V_{\text{xc}}^{\text{KSG}}$ for the clean Al calculation. This yields a work function of (3.7 ± 0.1) eV, which underestimates the Grepstad *et al.*[1] experimental value of (4.41 ± 0.03) eV. In a self-consistent surface calculation for the W(100) surface,[20] it was found that additional explicit terms for correlation were needed to yield a work function in agreement with experi-

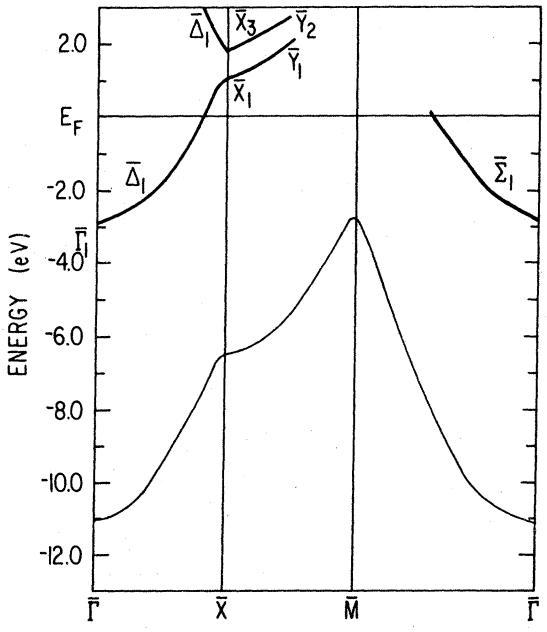

FIG. 2. Surface states and surface resonances for clean Al(001). The bottom of the Al valence band is outlined along the lower portion of the figure.

ment. The surface dipole barrier, by definition, forms in a region where $\rho(\vec{r})$ varies rapidly. It is not surprising, therefore, that correlation terms—which can be expressed as a density-dependent exchange coefficient $\alpha[\rho(\vec{r})]$—are important in yielding a correct dipole barrier. Hence the self-consistent calculations were repeated for the clean Al(001) surface using the Wigner interpolation formula[20,25] for the correlation contribution to V_{xc}. This yields a work function (4.7 ± 0.1) eV which is in better agreement with experiment, and parallels our experience with the W(100) surface.[20] (Lang and Kohn[22] obtained a jellium work function of 4.2 eV for this surface using the Wigner interpolation formula.) By contrast the energy bands and bonding characteristics of $\rho(\vec{r})$ are essentially identical to those obtained using V_{xc}^{KSG}, again paralleling our experience with the W(100) surface.[20] We did not, therefore, repeat the calculations for the oxygen-covered Al(001) surface using the Wigner interpolation formula.

B. Band structure

The surface states and surface resonance states for the clean Al surface are presented in Fig. 2.

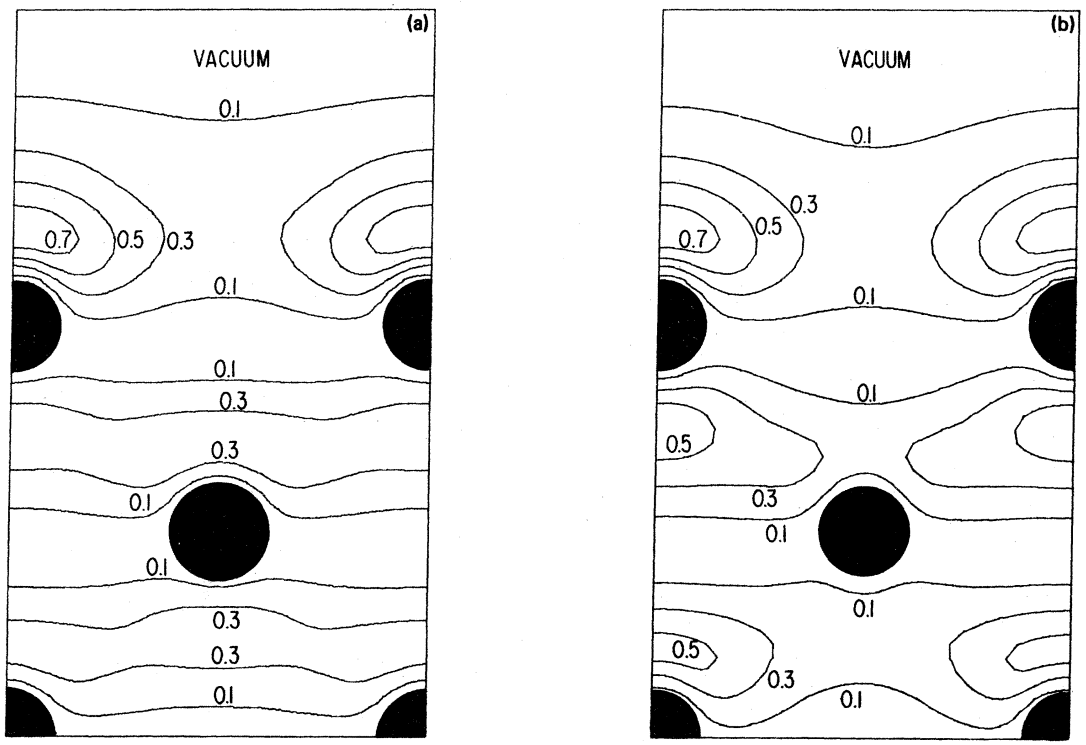

FIG. 3. Contour plots of the charge density for (a) the clean Al surface state at $\bar{\Gamma}$, and (b) the clean Al surface resonance state midway between $\bar{\Gamma}\bar{X}$. Successive contours differ by 0.2 in units of electrons per bulk Al unit cell.

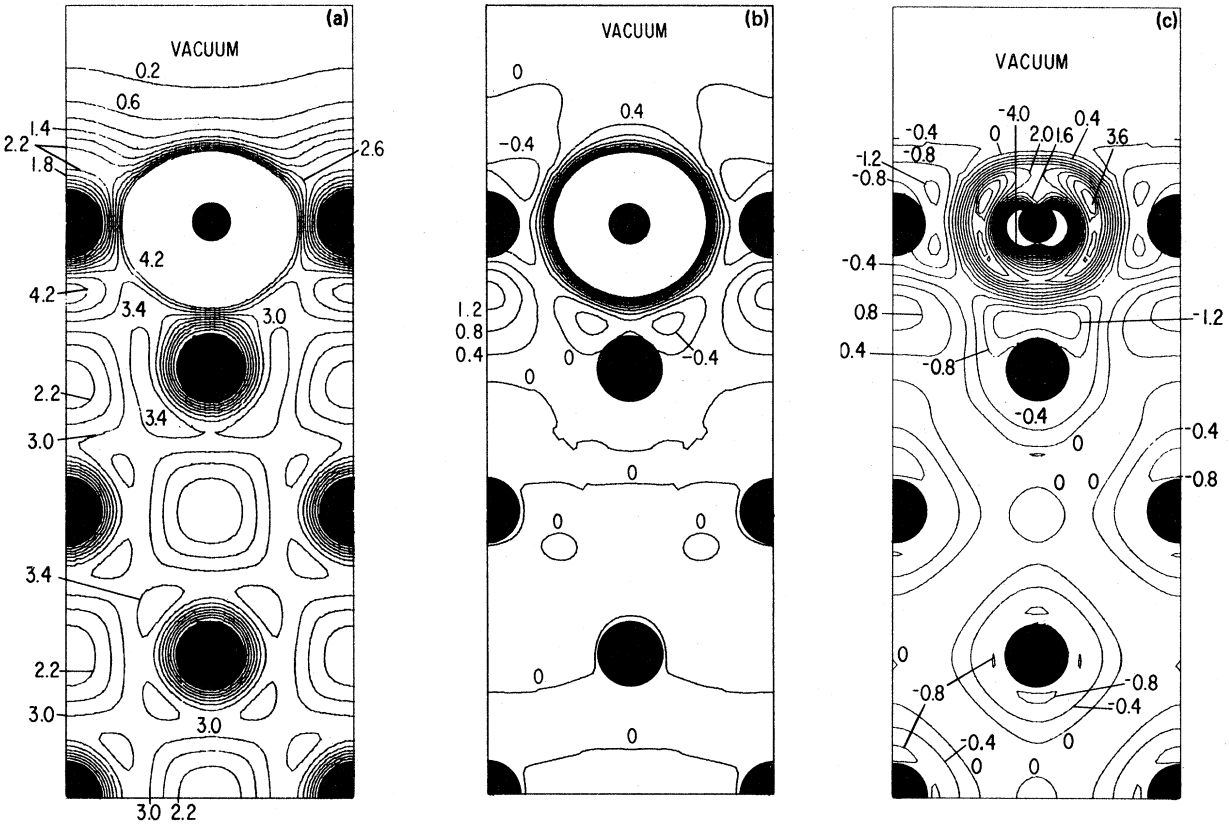

FIG. 4. Contour plots of (a) the self-consistent total valence charge density for the upper half of the Al(001)/O slab, (b) the difference between the Al(001)/O self-consistent total charge density and that for clean Al(001), and (c) the difference between the Al(001)/O self-consistent total charge density and the non-self-consistent starting charge density (constructed as a superposition of overlapping spherical atomic charge densities) for the Al(001)/O slab. Successive contours differ by 0.4 in units of electrons per bulk Al unit cell.

The large number of bulklike Al states have been suppressed for greater clarity of presentation. For reference the bottom of the film-derived Al-conduction band is indicated by the thin solid line along the lower portion of the figure. A good measure of the ability of the nine-layer Al film to reproduce the bulk electronic structure is given by the total occupied bandwidth, i.e., the distance between the Fermi energy E_F and the conduction-band minimum. Our value (11.07 eV) is in excellent agreement with the fully self-consistent bulk results of Singhal and Callaway[26] (11.1 eV).

Surface states for clean Al(001) were first reported in a non-self-consistent pseudopotential calculation by Caruthers, Kleiman, and Alldredge,[27] and the existence and nature of surface resonance states (i.e., surface localized states which have finite amplitude deep inside the bulk) were first discussed by us in a non-self-consistent LAPW calculation.[28] The inclusion of self-consistency does not have a significant effect on the surface states and resonances found earlier. Both the $\bar{\Delta}_1$ and $\bar{\Sigma}_1$ states in Fig. 2 are in good agreement with angular resolved photoemission measurements.[29,30] We also find some unoccupied surface states above E_F in Fig. 2. Contour plots for the $\bar{\Delta}_1$ state are shown in Fig. 3. Figure 3(a) shows the true surface state at $\bar{\Gamma}_1$, and Fig. 3(b) shows the $\bar{\Delta}_1$ state midway between $\bar{\Gamma}$ and $\bar{X}$, where it is a surface resonance state. The similarity of these contour plots is consistent with earlier conclusions regarding the origin of surface resonance states in nearly-free-electron metals.[28]

C. Surface core-level shifts

In agreement with recent measurements[31] on the Al(2p) core level, we find no surface core-level shift of the Al core levels relative to an interior atom. Upon chemisorption of oxygen, how-

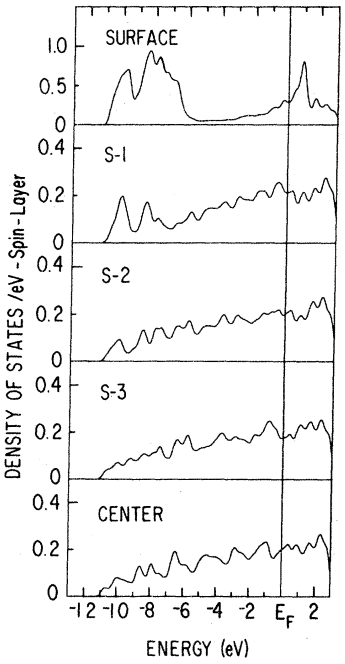

FIG. 5. Layer projected density of states for the Al(001)/O slab. Note the change of scale for the surface layer density of states.

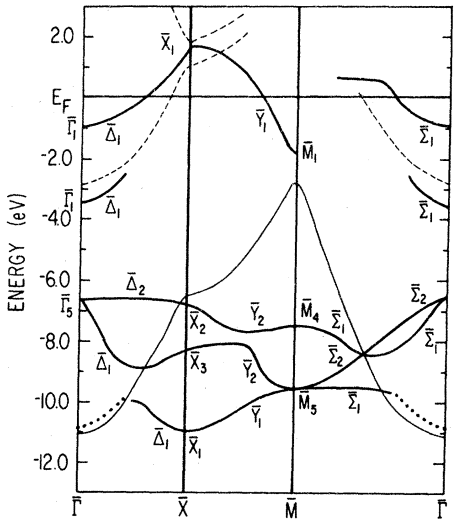

FIG. 6. Surface states and surface resonance states for the Al(001)/O slab. The dashed lines represent the surface states for the clean Al(001) slab. The bottom of the Al valence band is traced as in Fig. 2. The dotted lines are discussed in the text.

ever, we obtain sizable chemical shifts, as discussed in the next section.

Although no surface-induced shift of the Al $2p$ binding energy was observed in Ref. 31, a broadening (~0.2 eV) of the surface core level relative to a bulk level was observed (a similar broadening was also observed in Ref. 31 for Au). To explain this broadening, Eberhardt *et al.*[31] invoked a crystal field splitting of the surface Al $2p$ core level due to the reduced symmetry at the surface. In order to examine this possibility, we recalculated all the Al($2p$) core levels as band states at several $\vec{k}$ points in the 2D Brillouin. Within the accuracy of the calculated eigenvalues (1–3 mRy) no dispersion was obtained for these states and no evidence for a crystal field splitting was found. Our results may not be conclusive, however, since the present calculation neglects nonspherical components of the potential inside the muffin-tin spheres, although the full potential is correctly treated everywhere else. As the Al($2p$) core states have negligible amplitude outside the muffin-tin spheres, the neglected nonspherical terms may be essential in determining any crystal field splitting. Work is currently underway to include these neglected terms (i.e., the full potential will be treated with no shape approximations whatsoever).

IV. RESULTS FOR THE Al(001)-O SURFACE

A. Charge density and work-function changes

We first present the self-consistent charge density and discuss the bonding of the chemisorbed O atoms to the substrate and the resulting change in the work function compared to the clean Al surface. Figure 4(a) presents a contour plot of the total valence charge density [including the O($2s$) state which was calculated as a band state], and Fig. 4(b) shows the difference between the (SC) Al–O charge density and the SC clean Al $\rho(r)$ (Fig. 1). Another useful difference plot is given by Fig. 4(c) which displays the difference between the SC Al–O charge density and the initial-model charge density constructed as a superposition of overlapping spherical atomic charge densities. Many densely spaced contours corresponding to large values of O charge density have been suppressed around the O atom in Figs. 4(a) and 4(b). In Fig. 4, the large circles locate the Al atoms and the small circles locate the O atoms. Such contour plots can provide physical insight into the nature of the chemical bonding. Upon going in towards the center of the film in Fig. 4(a), the charge density becomes essentially identical to its bulk value by the third layer in from the surface. Near the center of the film the bonding is essentially identical to that exhibited by the clean Al surface (Fig. 1). This is emphasized by the

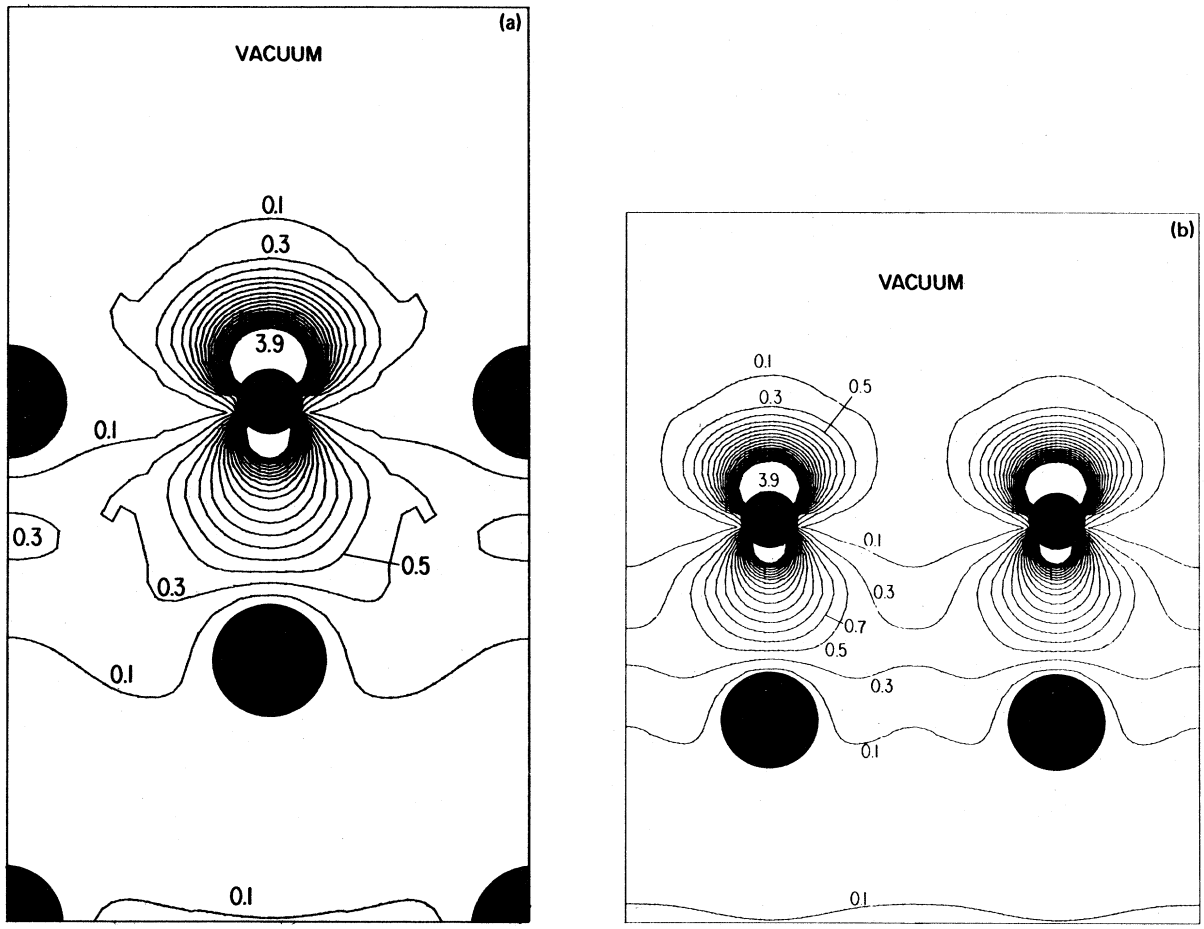

FIG. 7. Contour plot of the charge density for the $\bar{\Gamma}_1$ O($2p$) state (a) in a (110) plane and (b) in a (010) plane. Successive contours differ by 0.2 in units of electrons per bulk Al unit cell. This figure has unusually large discontinuities at the MT radius of the neighboring Al atoms.

difference contour plot in Fig. 4(b) which reveals only very small changes in the interior of the nine-layer Al slab. To fully appreciate the significance of this surface screening effect, compare Figs. 4(b) and 4(c). The superposition charge density [Fig. 4(c)] exhibits substantial differences throughout the slab, but after achieving self-consistency for both the clean and oxygen-covered surfaces, only minimal differences are in evidence in Fig. 4(b). Thus the nine-layer slab of Al is seen to be completely adequate for treating *both* the bulk and surface electronic structure for the oxidized surface.

Between the second and third layer in from the surface, however, departures from bulk behavior become apparent in Fig. 4. The second-layer Al atom and especially the surface Al atom show marked changes in the charge density, reflecting the strong influence of the neighboring O atom in the surface layer. It is apparent from Figs. 4(b) and 4(c) that the bonding is largely ionic in nature, i.e., the radius of the nearly spherical charge density centered on the O atom (~1.3 Å) in Fig. 4(b) is quite close to the ionic radius of O^{-2}, 1.4 Å.[32] Another interesting feature in Figs. 4(b) and 4(c) is the pileup of bonding charge just below the Al surface layer. This feature is also apparent in Fig. 4(a), reaching a maximum of about 4.2 electrons per cell. The pile-up of electrons below the surface Al atom is accompanied by a depletion of electronic charge just above the surface Al atom. This results in the formation of a dipole moment (opposing the usual surface dipole layer) which tends to reduce the work function as compared to that for the clean Al surface, as discussed below.

Another effect of the charge transfer onto the O atom is that the O($2p$) states experience an in-

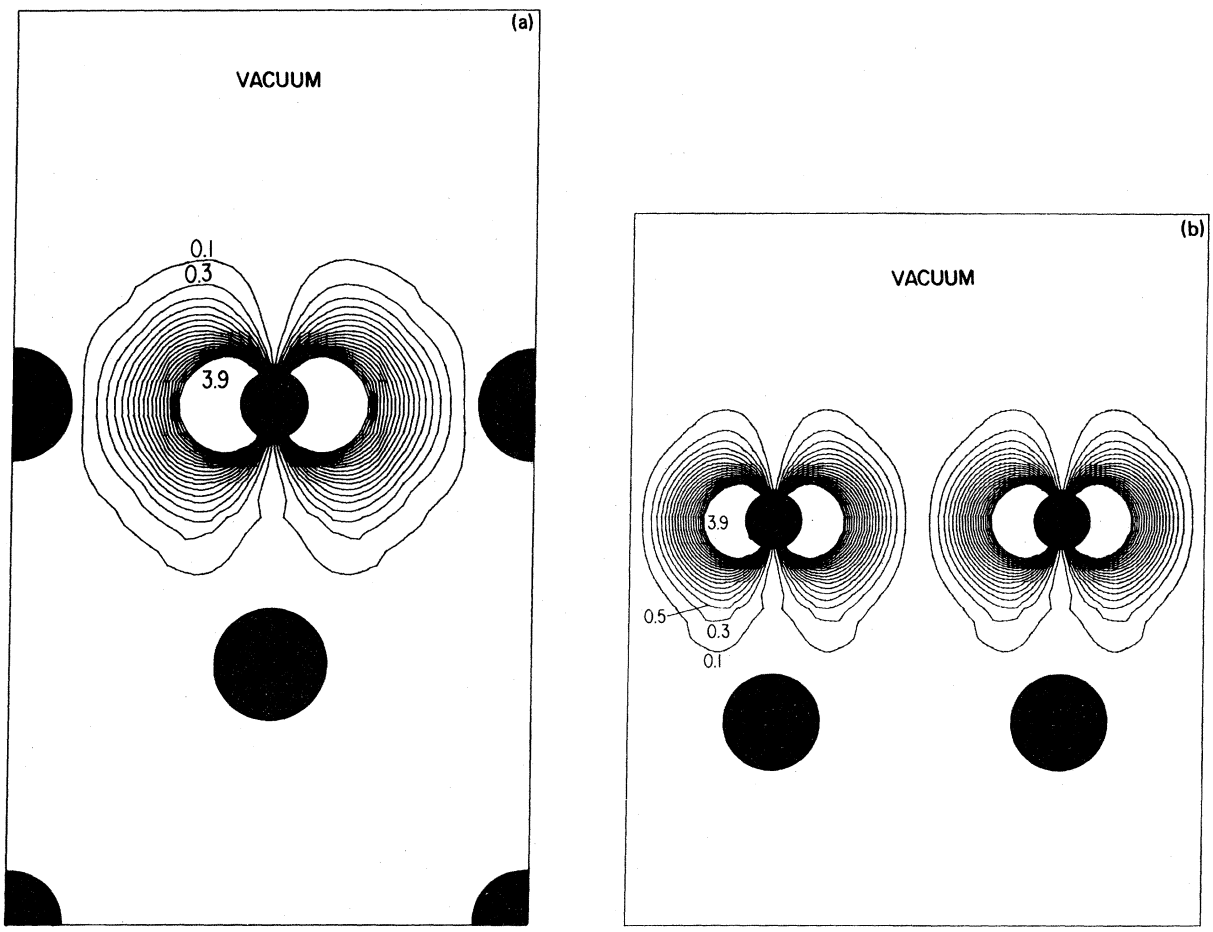

FIG. 8. Contour plot of the charge density for the $\bar{\Gamma}_5$ O($2p$) state (a) in a (110) plane and (b) in a (010) plane. Successive contours differ by 0.2 in units of electrons per bulk Al unit cell.

creased screening of the O nucleus. This results in the expansion of the O($2p$) density which is strikingly pictured in Fig. 4(c) for the O(p_x,p_y) states (i.e., the contours near the O nucleus have large negative values, indicating the movement of electrons away from the nucleus compared to the free atom). In addition, the downward bulging of the contours below the O atom in Fig. 4(c) reveals the expansion of the O($2p_z$) states as well as the effects of interaction with the substrate.

The substantial change in the surface charge density between the clean surface and the O-covered surface, leads to a reduction in the work function of Al(001)/O as compared to Al(001) by 0.6 eV [both calculated using the KSG (Ref. 22) V_{xc}]. This value is in good agreement with the O-saturated value of 0.5–0.8 eV for the Al(001) surface.[1] This is a significant result, since the saturation change in work function on Al(110) and Al(111) surfaces is only of the order of about 0.1 eV.[1,2] Thus, the anomalous behavior of the work function for the (001) surface is seen to be associated with (1) the open structure of the (001) surface which permits the O atom to be incorporated into the fourfold hollow site in a *coplanar* position with respect to the Al surface atoms [coplanar absorption seems unlikely in the hollows of the more open (110) surface, as this would require a 1.43 Å Al–O bond length between the O atom and the subsurface Al atom—a value much smaller than the shortest bond length, 1.86 Å,[32] in bulk Al_2O_3], and (2) the large charge transfer onto the O atom and the accompanying formation of a dipole moment localized on the surface Al atom [Fig. 4(b)] which opposes the usual surface dipole barrier formed on the clean Al surface. All of these results are consistent, therefore, with earlier suggestions that the O atoms are adsorbed into the fourfold hollow sites of the surface layer.

B. Density of states

An overview of the electronic structure for the O-covered surface is given by the layer-by-layer

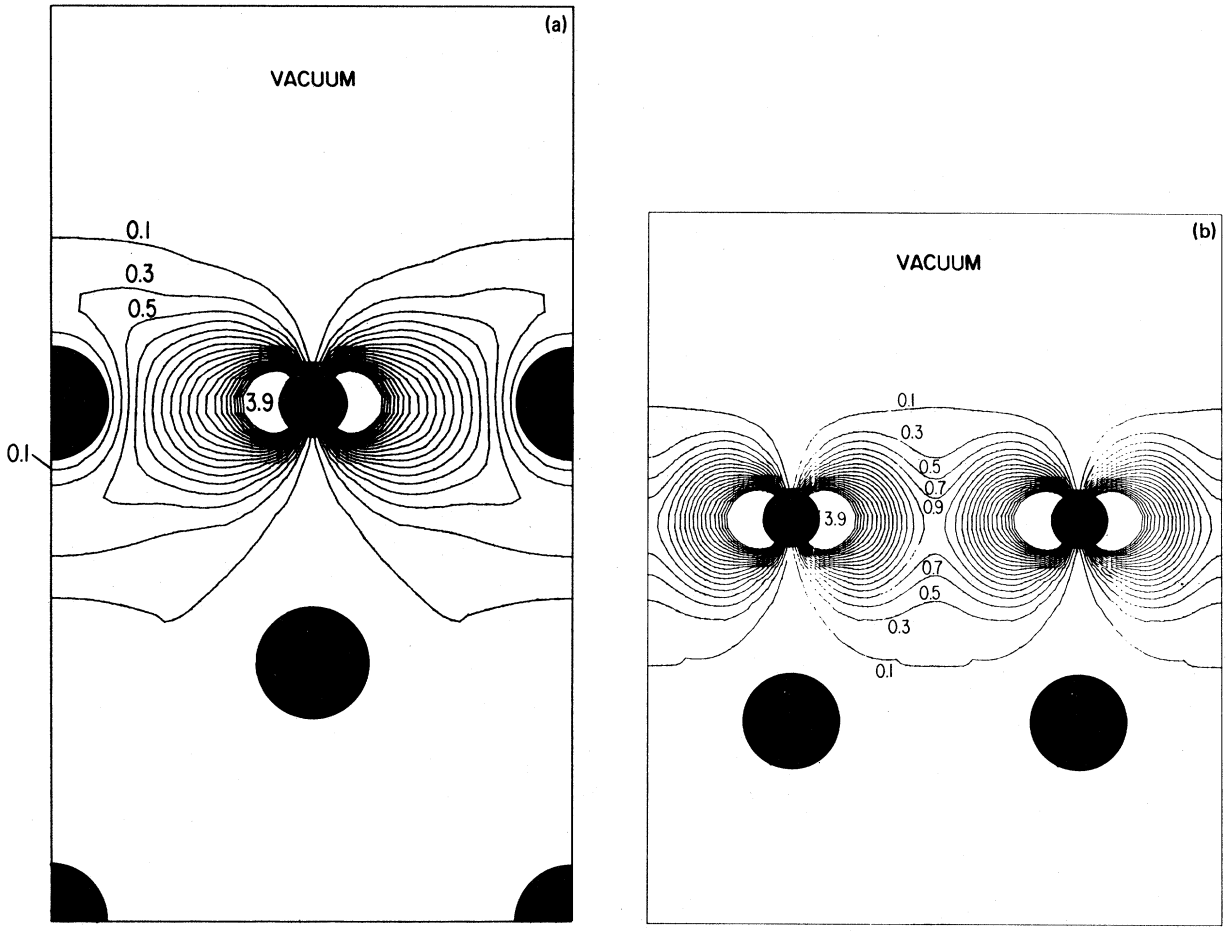

FIG. 9. Contour plot of the charge density for the $\overline{X}_1$ O($2p$) state (a) in a (110) plane and (b) in a (010) plane. Successive contours differ by 0.2 in units of electrons per bulk Al unit cell.

density of the states (DOS) present in Fig. 5. Since the O atoms are located precisely on the Al surface layer, there are five layers going from the center of the film out towards the surface (note the change of scale in the top panel of Fig. 5). Each of the layer-projected DOS curves shown in this figure has been smoothed with a Gaussian of full width at half maximum equal to 0.3 eV.

The overall shape of the DOS for the innermost layers is parabolic, as is expected for a nearly-free-electron substrate metal like Al. There are prominent peaks in the surface layer DOS at about −8.0 and −10.0 eV below the Fermi energy E_F which are due to the O($2p$) bands. The overall width of the O($2p$) bands is seen to be about 3.5 eV, and the split peak structure indicates a crystal field splitting of the O($2p$) states. That this is indeed the case is discussed in detail in Sec. IV C. These peaks are in good agreement with photoemission measurements.[5,7] In addition to this structure, there are narrow peaks in the surface DOS above E_F. These structures are related to unoccupie oxygen-induced surface resonance states. We believe that they correspond to the unoccupied interface DOS at ~1.0 eV above E_F and a smaller peak ~1.8 eV states (S_1 and S_2 in Refs. 9 and 14) observed by surface soft-x-ray absorption (SSXA) spectroscopy. All of these oxygen-related structures are superimposed on the parabolic Al background DOS. In the first layer in from the surface ($S-1$ in Fig. 5), the oxygen-related structures are greatly reduced in magnitude, and they have nearly vanished by layer $S-2$, reflecting the surface-localized nature of the chemical bond between the O atoms and the Al substrate. This behavior is also reflected in the rapid healing of the charge density to bulk Al character shown in Fig. 4. Not shown in Fig. 5 is the O($2s$) state which is located at 23.2 eV below E_F (experimentally it is located at −25.0 eV). As stated before, this state was treated as a valence state in the calculations and was found to have an overall dispersion of 1.1 eV.

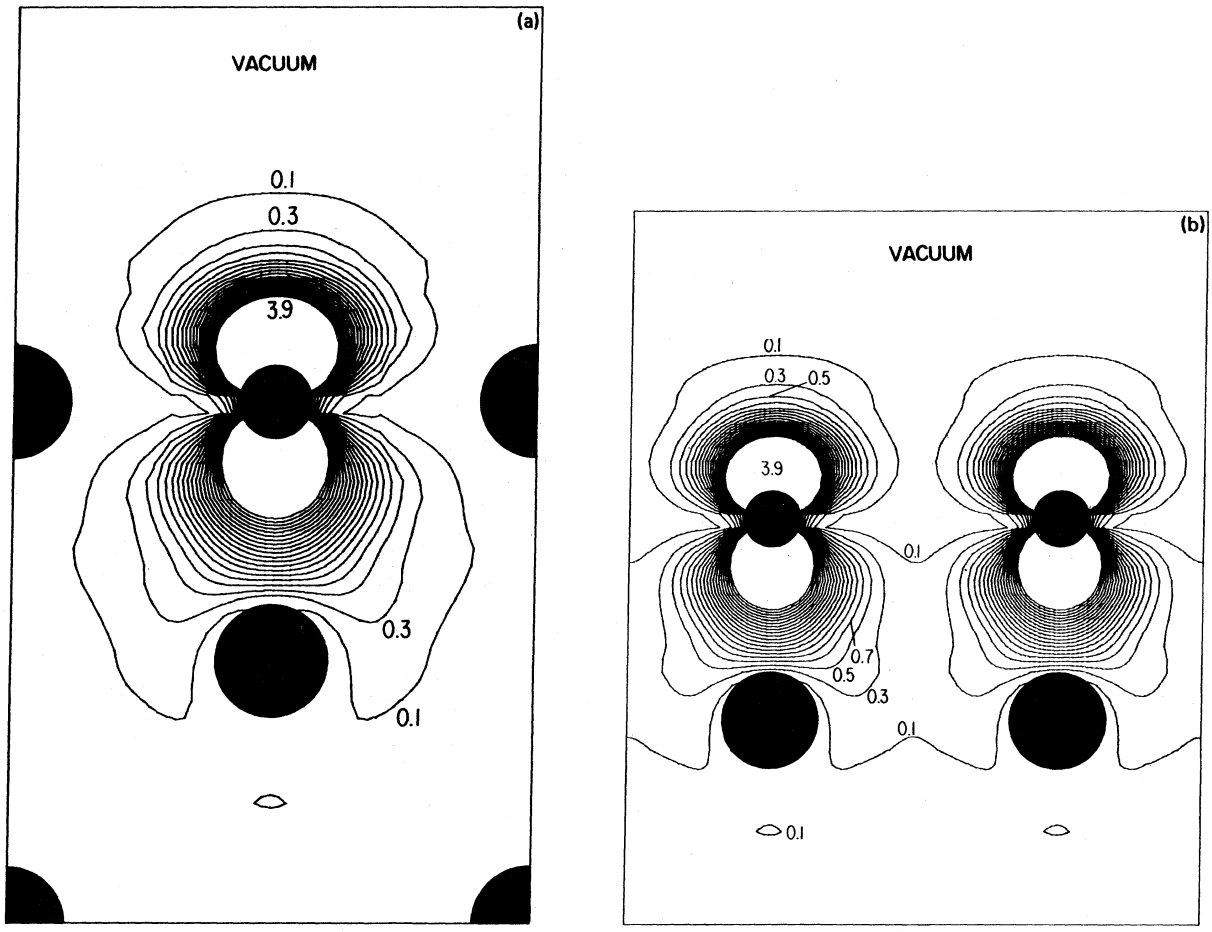

FIG. 10. Contour plot of the charge density for the $\bar{X}_3$ O($2p$) state (a) in a (110) plane and (b) in a (010) plane. Successive contours differ by 0.2 in units of electrons per bulk Al unit cell.

C. Band structure

The band structure of states localized near the surface is presented in Fig. 6. The heavy solid curves in this figure show the surface states and surface resonances for Al(001)-O along the symmetry lines of the 2D square Brillouin zone (BZ). Only those states which have a localization of at least 60% in the first two surface layers are shown (recall that the O atoms lie precisely in the surface layer). Thus the large number of bulklike Al conduction states have been suppressed, as in Fig. 2, for greater clarity. For reference, the bottom of the film-derived Al conduction band is again indicated by the thin solid line along the lower portion of the figure. The dashed-line curves show the surface states and surface resonances from Fig. 2 for the clean nine-layer Al(001) film (E_F for both films have been made to coincide in this figure). The dotted lines are discussed below.

1. Oxygen (2p) states

We first focus on the O($2p$) derived bands in Fig. 6. As expected, these states are very localized (typically 90%) in the surface layer. The center of gravity of these states is about 8.5 eV below E_F, and their overall width is about 3.0 eV. They are thus well separated in energy from the other localized states shown in Fig. 6. Inspection of Fig. 6 shows that while there is some overlap with the Al conduction-band states, there are large regions of the 2D BZ where the O($2p$) bands lie well below the energy range of the substrate states. In these regions of the 2D BZ the O($2p$) bands are very well localized true surface states. As a result of the overlap near the $\bar{\Gamma}$ point, however, the lowest-lying O($2p$) $\bar{\Gamma}_1$ and $\bar{\Sigma}_1$ bands mix strongly with the Al conduction states, resulting in a reduced surface localization (50–60%). The continuation to $\bar{\Gamma}$ of the lowest-lying $\bar{\Delta}_1$ and $\bar{\Sigma}_1$

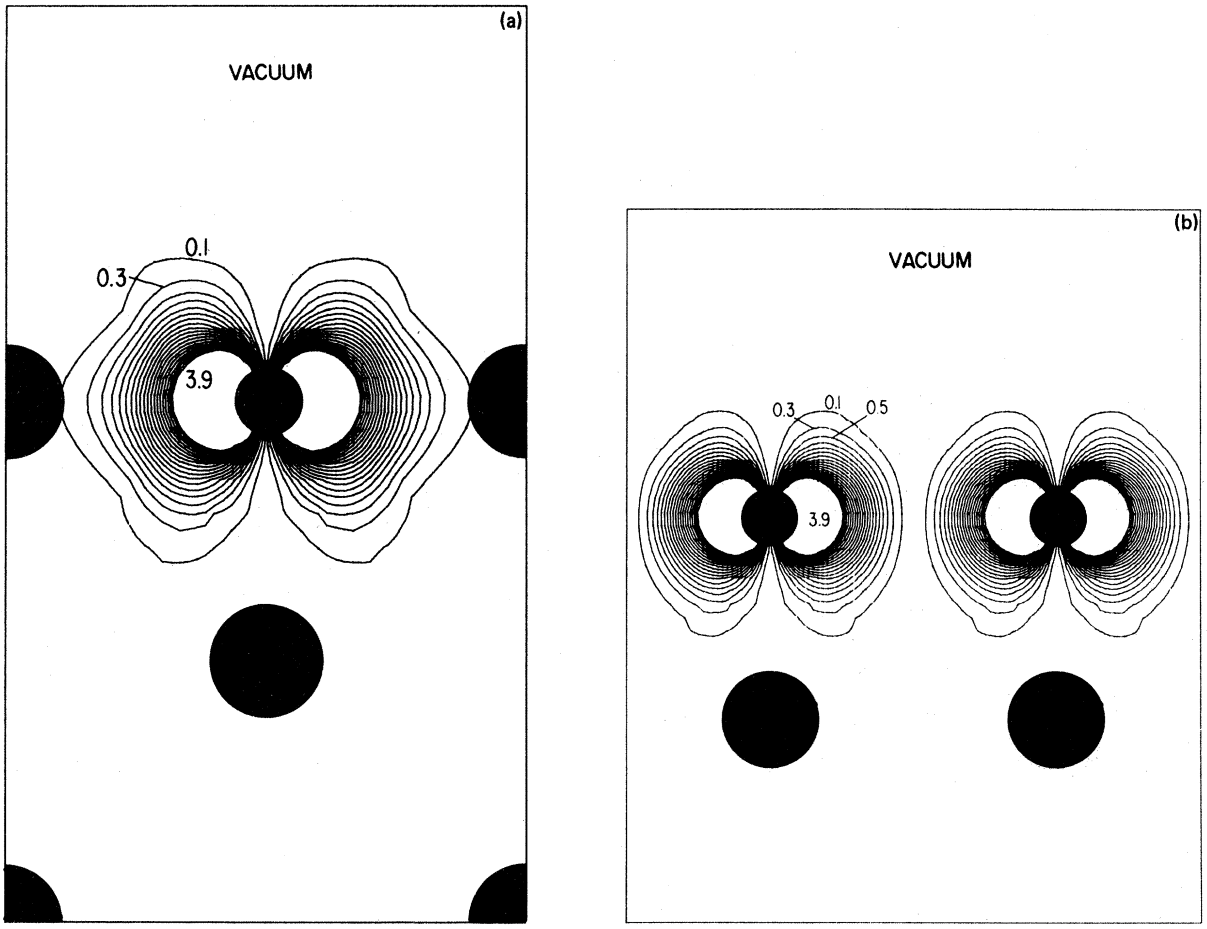

FIG. 11. Contour plot of the charge density for the $\bar{X}_2$ O($2p$) state (a) in a (110) plane and (b) in a (010) plane. Successive contours differ by 0.2 in units of electrons per bulk Al unit cell.

bands is, therefore, represented in Fig. 6 by the dotted-line curves. Since the Al conduction bands in the energy region of the overlap all belong to the fully symmetric representations ($\bar{\Gamma}_1$, $\bar{\Delta}_1$, and $\bar{\Sigma}_1$), the $\bar{\Gamma}_5$, $\bar{\Delta}_2$, and $\bar{\Sigma}_2$ O($2p$) states are strictly orthogonal to the substrate states and can be thought of as very localized true surface states on these symmetry lines. The upper O($2p$) $\bar{\Delta}_1$ and $\bar{\Sigma}_1$ states remain very localized in the surface layer, however, even in the regions where they are overlapped by Al conduction bands of the same 2D symmetry. In these regions of the 2D BZ, they are very localized surface resonance states and not true surface states.

The reason for the different behavior between the two O($2p$) $\bar{\Delta}_1$ bands and between the two O($2p$) $\bar{\Sigma}_1$ bands can be traced to the orbital character of these bands. The $\bar{X}_1$ state at -11.0 eV has O($2p_{x,y}$) character (i.e., lobes directed parallel to the surface) as does the doubly degenerate $\bar{M}_5$ state at about -9.5 eV, while the $\bar{X}_3$ state and the $\bar{M}_4$ state have O($2p_z$) character. Moving away from $\bar{X}$ towards $\bar{\Gamma}_1$, the lowest $\bar{\Delta}_1$ state begins to acquire some O($2p_z$) character and the upper $\bar{\Delta}_1$ state begins to acquire some O($2p_{x,y}$) character. Similarly, the lowest $\bar{\Sigma}_1$ state begins to acquire O$p2p_z$) character as one moves from $\bar{M}$ to $\bar{\Gamma}$, and the upper $\bar{\Sigma}_1$ state begins to acquire some O($2p_{x,y}$) character. At about the midway point of the $\bar{\Gamma}\bar{X}$ line and the $\bar{\Gamma}\bar{M}$, respectively, both $\bar{\Delta}_1$ states and both $\bar{\Sigma}_1$ states have about equal components of O($2p_{x,y}$) and O($2p_z$) character. These correspond to "anticrossings" of the two O($2p$) $\bar{\Delta}_1$ bands along $\bar{\Gamma}\bar{X}$ and the two O($2p$) $\bar{\Sigma}_1$ bands along $\bar{\Gamma}\bar{M}$. Continuing towards $\bar{\Gamma}_1$, the O($2p_z$) character becomes rapidly predominant in the lowest $\bar{\Delta}_1$ and $\bar{\Sigma}_1$, while the upper O($2p$) $\bar{\Delta}_1$ and $\bar{\Sigma}_1$ are predominantly of O($2p_{x,y}$) character near $\bar{\Gamma}$. A similar anticrossing, where O($2p_z$) character and O($2p_{x,y}$) character are exchanged, occurs between the two $\bar{Y}_2$ bands midway along the $\bar{X}\bar{M}$ line. The surface delocalization of the lowest $\bar{\Delta}_1$ and $\bar{\Sigma}_1$ bands is

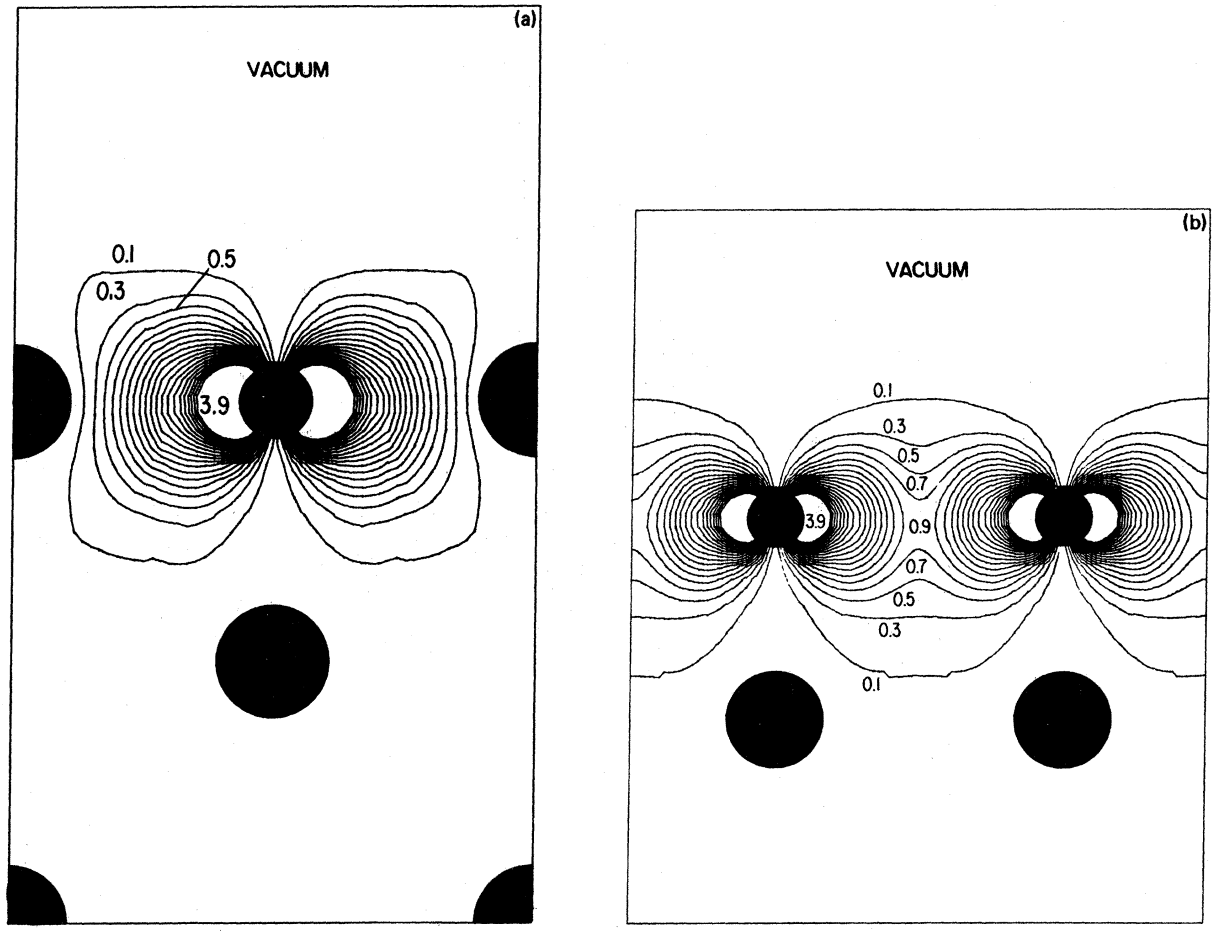

FIG. 12. Contour plot of the charge density for the $\bar{M}_5$ O($2p$) state (a) in a (110) plane and (b) in a (010) plane. Successive contours differ by 0.2 in units of electrons per bul'- Al unit cell.

thus associated with increasing O($2p_z$) character occurring in a region of the 2D BZ where these states are overlapped by Al conduction states. The O($2p_z$) states have lobes pointing downward into the bulk, facilitating hybridization with the substrate states (Fig. 7). By contrast, the upper Op2p) $\bar{\Delta}_1$ and $\bar{\Sigma}_1$ bands near $\bar{\Gamma}$ have O($2p_{x,y}$) symmetry and lobes pointing parallel to the surface, resulting in less hybridization with the substrate states (Fig. 8).

Batra and Ciraci[18] have performed a non-self-consistent calculation for an eight-layer Al(001) film plus a monolayer of (1×1)O located in the fourfold hollow site on one of the slab surfaces. There are many qualitative and quantitative differences between their calculation and the present one: (a) Unlike our value of 11.07 eV, which is in agreement with the bulk Al result, the occupied overall bandwidth in Ref. 18 is about 14.6 eV. (b) The O($2p$) states in Ref. 18 overlap the Al conduction-band states everywhere in the 2D BZ except a small pocket around $\bar{M}$ (denoted K in Ref. 18). (c) Batra and Ciraci find that the O($2p_z$) character is dispersed in a large energy range extending from E_F to about −6 eV, and essentially loses its identity due to hybridization with the Al conduction states. These differences indicate the importance of self-consistency.

In order to study more closely the orbital character and bonding nature of the low-lying O($2p$) states, contour plots for these states at the high symmetry points of the 2D BZ are shown in Figs. 7–13. In these instructive plots, as well as those which follow, only the outer three layers of the film are shown. As before, the large solid circles indicate the position of the Al atoms and the small solid circles indicate the O atom position. All the contour plots are in vertical planes which are perpendicular to the surface. For the low-lying O($2p$) states, contours in two vertical planes are shown: a $(110)_s$ and a $(100)_s$ plane, with the s subscript denoting that these directions are with

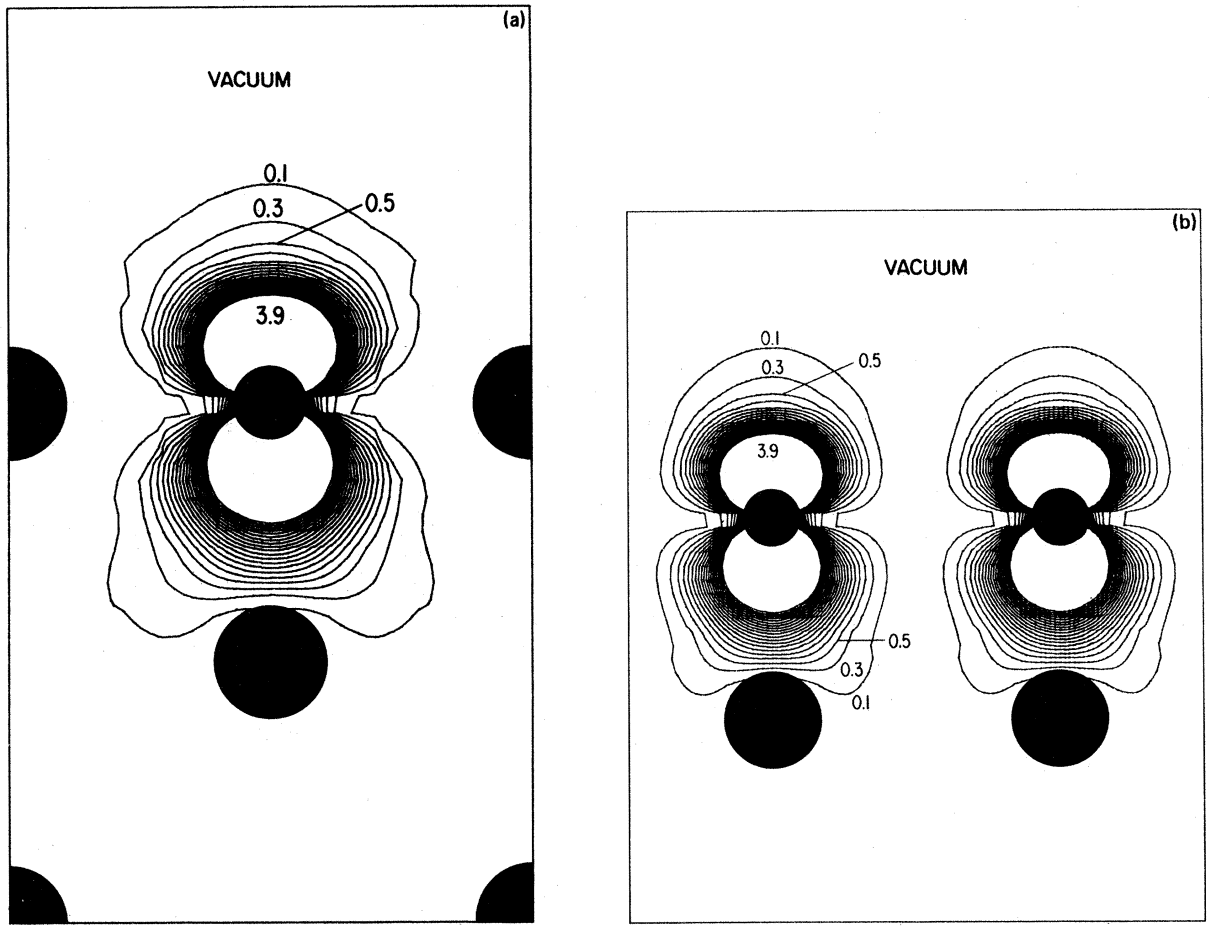

FIG. 13. Contour plot of the charge density for the $\bar{M}_4$ O($2p$) state (a) in a (110) plane and (b) in a (010) plane. Successive contours differ by 0.2 in units of electrons per bulk Al unit cell.

respect to the 2D square lattice. The $(110)_s$ plane is equivalent to a $(100)_{\text{Bulk}}$ plane with respect to the 3D lattice, and the $(100)_s$ plane is equivalent to a $(100)_B$ plane. The $(110)_s$ cuts highlight the O–Al interactions, while the $(100)_s$ cuts highlight O–O interactions. At the selected k points the charge density corresponding to the star of the $\tilde{k}$ point is plotted, so that all the contour plots have the full crystal symmetry.

Figure 7 plots the charge density for the O($2p_z$) state −11.0 eV below E_F at $\bar{\Gamma}_1$ in Fig. 6. As noted above, its interaction with the substrate Al states results in reduced surface localization, although its $2p$ orbital character on the O atom is still retained. Figure 7(b) reveals some overlap with neighboring O atoms. As a result of its interactions with the substrate, this is the most tightly bound O($2p$) state at $\bar{\Gamma}$.

Figure 8 plots the doubly degenerate O(p_x, p_y) state at $\bar{\Gamma}_5$. These states are essentially atomiclike with little interaction with Al or other O atoms. This results in a splitting of over 4.0 eV at $\bar{\Gamma}$ between these O(p_x, p_y) states and the lower-lying O(p_z) state.

Figure 9 plots the bonding O($p_{x,y}$) state ($\bar{X}_1$ in Fig. 6). This state reveals substantial σ bonding to neighboring O atoms as well as to the surface Al atom. There is essentially no interaction with the surface minus one ($S-1$) layer Al atom. This is the lowest-lying O($2p$) state at $\bar{X}$. Figure 10 shows the O(p_z) state at $\bar{X}_3$. It bonds to a lesser degree with the substrate and neighboring O atoms than does the $\bar{X}_1$ state in Fig. 9. Figure 11 plots the nonbonding O(p_x, p_y) state at $\bar{X}_2$. As can be seen from this figure, this state is essentially atomiclike. As a result, it is the highest lying of the O($2p$) derived bands at $\bar{X}$. Figure 12 plots the doubly degenerate O($2p_{x,y}$) state at $\bar{M}_5$. This state shows strong σ bonding to the other O atoms, but little interaction with Al atoms. Figure 13 plots the nonbonding O($2p_z$) state at M_4. This state shows little interaction with the other atoms, and

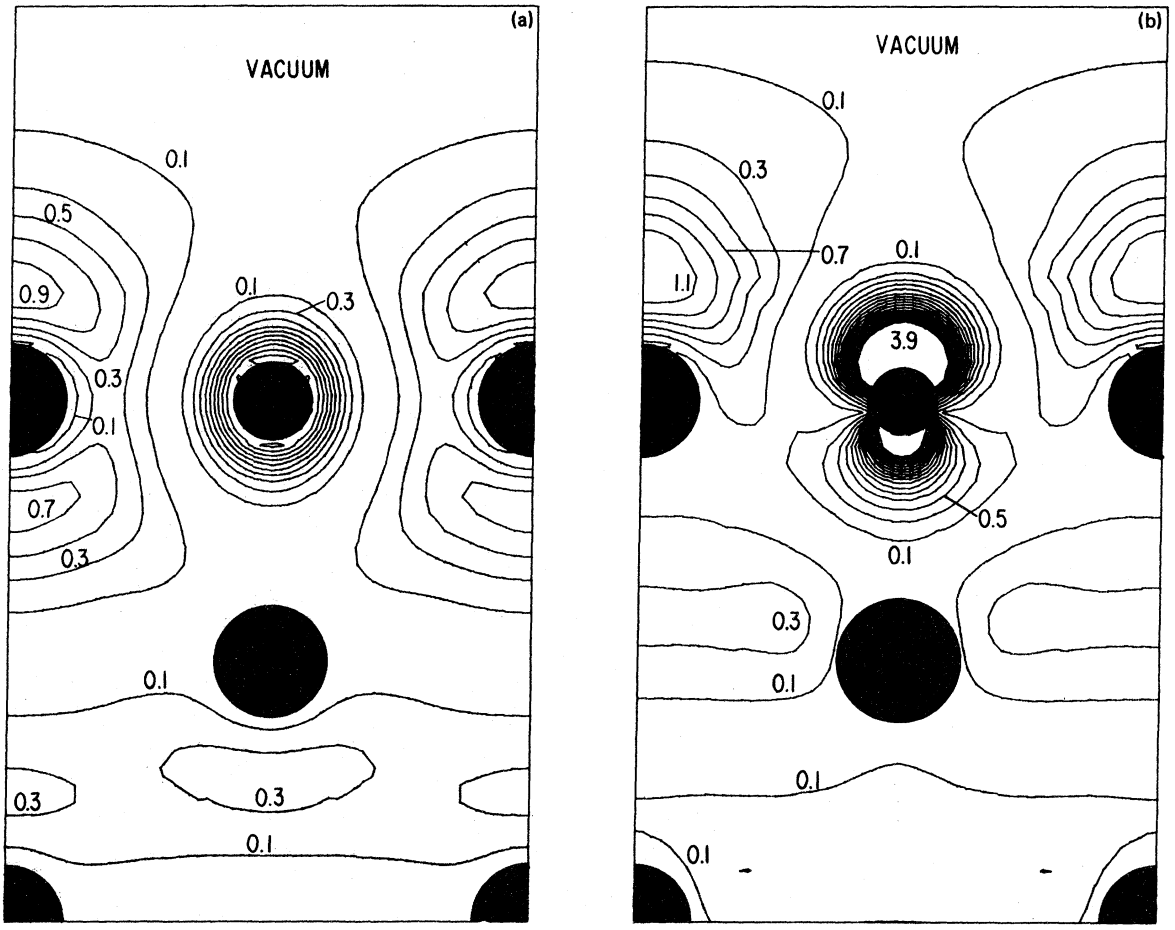

FIG. 14. Contour plot of the charge density in a (110) plane for (a) the −3.5-eV $\bar{\Gamma}_1$ oxygen-induced surface resonance and (b) the −1.0-eV $\bar{\Gamma}_1$ oxygen-induced surface resonance. Successive contours differ by 0.2 in units of electrons per bulk Al unit cell.

is the highest-lying O($2p$) derived band at $\bar{M}$. The resulting splitting at $\bar{M}$ is about 2.0 eV, which is smaller than at $\bar{\Gamma}$. In addition, it is the O($2p_{x,y}$) states which are lower at $\bar{M}$ while O($2p_z$) is lower at $\bar{\Gamma}$.

2. *Oxygen-induced surface resonance states*

In addition to the low-lying O($2p$) bands, there are higher-lying O-induced surface resonances shown in Fig. 6. The parabolic surface-state and surface resonance (SS-SR) bands in clean Al, going from about −3.0 eV at $\bar{\Gamma}$ up to $\bar{X}$ and up to E_F along $\bar{\Gamma}\bar{M}$, is shifted or replaced by two bands of O-induced SR of $\bar{\Delta}_1$ symmetry along $\bar{\Gamma}\bar{X}$ and two bands of O-induced SR of $\bar{\Sigma}_1$ symmetry along $\bar{\Gamma}\bar{M}$. At $\bar{\Gamma}$ these states have about the same degree of surface localization as the clean Al SS, but the lower-energy O-induced $\bar{\Delta}_1$ of $\bar{\Sigma}_1$ SR fades away upon leaving $\bar{\Gamma}$. By contrast, the upper $\bar{\Delta}_1(\bar{\Sigma}_1)$ O-induced SR becomes much more localized on leaving $\bar{\Gamma}$: above E_F the upper $\bar{\Delta}_1$ and $\bar{\Sigma}_1$ states are quite localized (70–90%) in the first two surface layers. The $\bar{Y}_1$ SR band which crosses E_F on going from $\bar{X}$ to $\bar{M}$ also has this degree of surface localization. We identify the highly localized unoccupied SR states near $\bar{X}_1$ and midway between $\bar{\Gamma}\bar{M}$ with the surface structures at 1.8 eV and 1.0 eV in Fig. 5, and with the S_1 and S_2 interface structures seen in the SSXA measurements.[9,14]

We are not aware of any angular resolved photoemission studies of the O-covered Al(001) surface with which to compare our theoretically determined SR dispersions. Photoemission at normal exit reveals,[29] however, that the clean Al(001) SS at $\bar{\Gamma}$ persists up to a coverage of 160 L, finally disappearing at a saturation coverage of 200 L. In this study,[29] there was no indication of structure corresponding to the upper O-induced $\bar{\Gamma}_1$ SR state at −1.0 eV below E_F. This behavior of the clean Al SS was interpreted in terms of the island

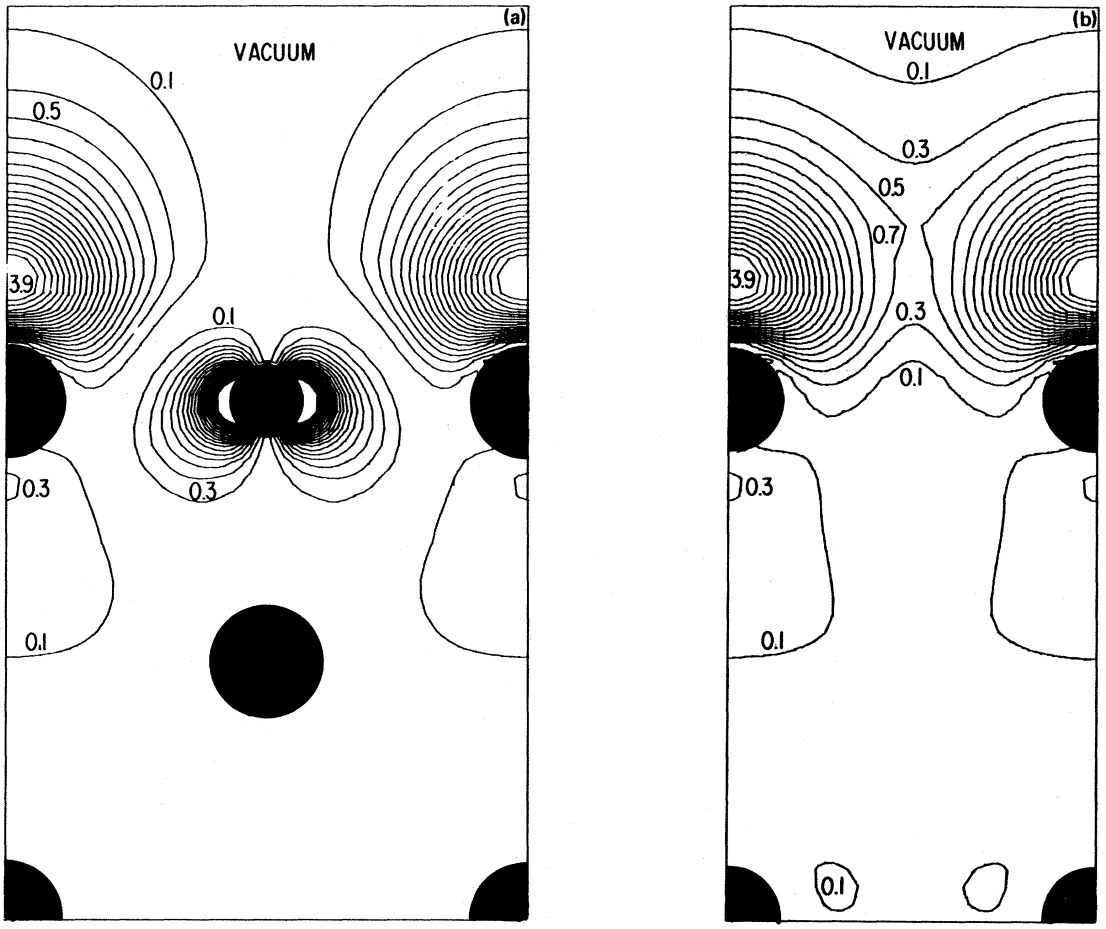

FIG. 15. Contour plot of the charge density for the unoccupied $\bar{X}_1$ oxygen-induced surface resonance (a) in a (110) plane and (b) in a (010) plane passing through the nucleus of the surface Al atom. Successive contours differ by 0.2 in units of electrons per bulk Al unit cell.

growth mechanism for the (001) surface,[1] i.e., since the areas of bare metal surface can exist right up to the point of saturation (150–200 L),[29] a SS may also exist up to these exposures. From Fig. 6 it is apparent that emission from the O-induced $\bar{\Gamma}_1$ state at −3.5 eV (which is near the bulk Al band edge[29]) may be increasing while emission from the clean Al SS is decreasing, thus complicating the interpretation[29] of the experimental result. Messmer and Salahub[16] also found evidence for oxygen-induced structure at 3.0 eV below E_F, and Batra and Ciraci[18] found bands with O($2p_z$) character at $\bar{\Gamma}$ about 2.0 eV and 3.2 eV below E_F which have parabolic dispersion up towards E_F along $\bar{\Gamma}\bar{X}$ and $\bar{\Gamma}\bar{M}$. Reference 18 does not, however, find the very localized O-induced SR $\bar{Y}$ band shown in Fig. 6.

Contour plots for the higher-lying O-induced SR states are shown in Figs. 14–16. Figure 14(a) shows the charge density for the $\bar{\Gamma}_1$ state at about −3.5 eV in Fig. 6, and Fig. 14(b) shows the charge density for the $\bar{\Gamma}_1$ state at about −1.0 eV in Fig. 6. For comparison, the clean Al $\bar{\Gamma}_1$ SS is shown in Fig. 3(a). All of these have about the same degree of localization in the two first surface layers. The largest angular momentum component on the O atom for the $\bar{\Gamma}_1$ SR in Fig. 14(a) is $l=0$ with a small admixture of p_z character. The orbital character on the O atom in Fig. 14(b) is almost entirely p_z-like. The fall off of the states as one approaches the center (bulk) part of the film shown in Fig. 14 is similar to those in Fig. 3 for the clean Al surface.

Figure 15 pictures the very localized unoccupied O-induced SR state at $\bar{X}_1$. This state is the continuation of the $\bar{\Gamma}_1$ state at −1.0 eV [Fig. 14(b)]. In Fig. 15, however, the Al(p_z) orbital is highly directed into a vacuum and there is very little interaction with Al atoms deeper into the slab. Figure 15 reveals some π bonding to neighboring

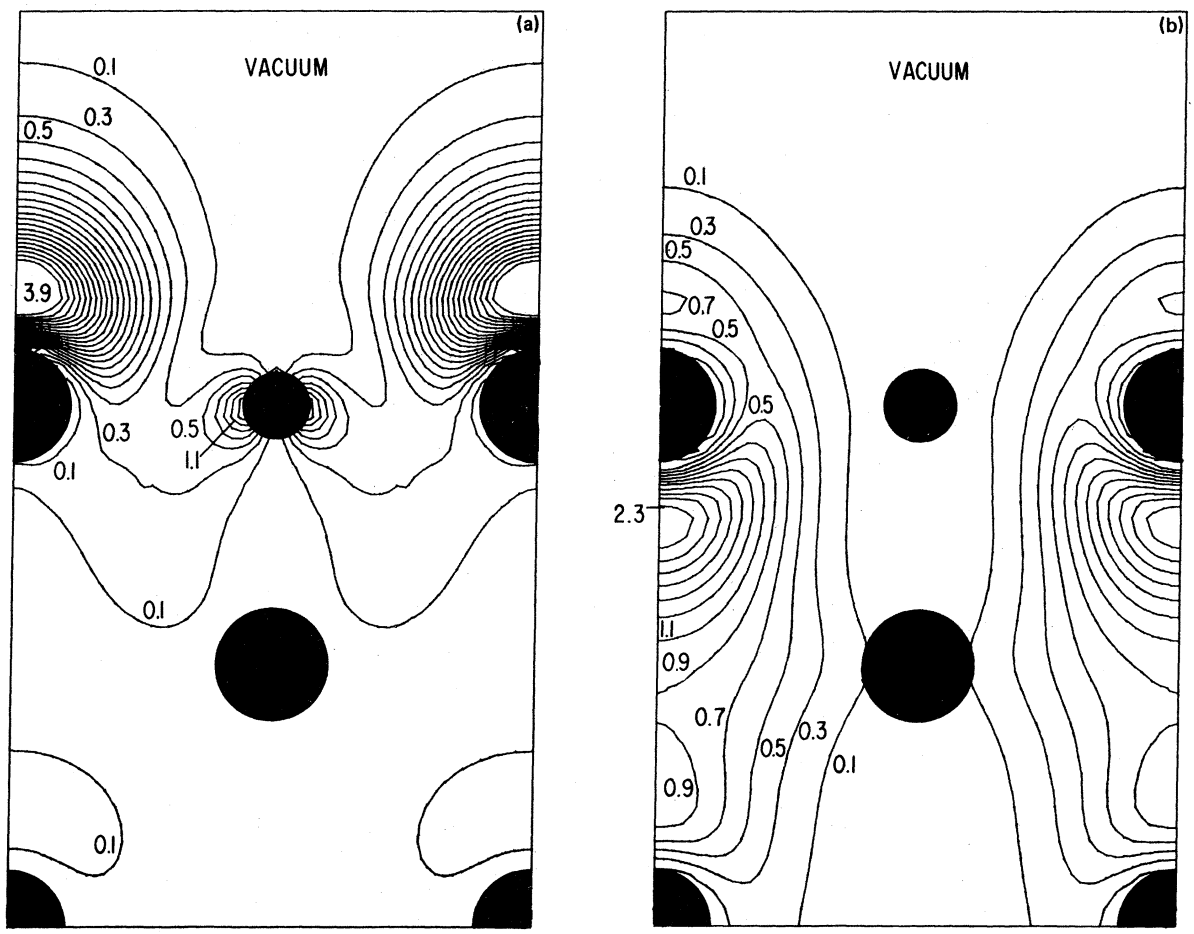

FIG. 16. Contour plot, in a (110) plane, of the charge density for (a) the unoccupied $\bar{Y}_1$ oxygen-induced surface resonance midway between $\bar{X}\bar{M}$, (b) the $\bar{M}_1$ oxygen-induced surface resonance, and (c) the unoccupied $\bar{\Sigma}_1$ oxygen-induced surface resonance midway between $\bar{\Gamma}\bar{M}$.

surface Al atoms. The principal orbital content on the O atom is $p_{x,y}$.

Figure 16(a) plots the very localized unoccupied SR state on the $\bar{Y}_1$ band (Fig. 6) midway between $\bar{X}\bar{M}$. This state is the continuation of the $\bar{X}_1$ state in Fig. 15 downward along the $\bar{Y}_1$ band and many similarities between these SR states are evident. There is substantially less interaction between the surface Al atom and the O atom and somewhat increased interaction with the other Al atoms.

Figure 16(b) plots the somewhat less localized (75%) SR state at $\bar{M}_1$ (Fig. 6), which is the further continuation of the states in Figs. 15 and 16(a) downward along the $\bar{Y}_1$ band. As can be seen in this figure, for this state there is essentially no overlap with the O atom. There is a drastic change on the surface Al atom as one proceeds from Fig. 15 to Figs. 16(a) and 16(b). The charge density no longer projects very far into the vacuum; instead there is a large pile-up of charge just below the surface Al atom and increased overlap with the $S-3$ Al atom.

Figure 16(c) shows the charge density for the unoccupied $\bar{\Sigma}_1$ band midway between $\bar{\Gamma}\bar{M}$ (Fig. 6). This state is the continuation of the $\bar{\Gamma}_1$ state at -1.0 eV (Fig. 6) along the $\bar{\Sigma}_1$ band, and its charge density is quite similar to the unoccupied $\bar{X}_1$ state shown in Fig. 15(a), which is the continuation of the -1.0 eV $\bar{\Gamma}_1$ state along the $\bar{\Delta}_1$ band.

As noted earlier, we believe the unoccupied $\bar{X}_1$ state shown in Fig. 15 (1.8 eV above E_F) and the unoccupied $\bar{\Sigma}_1$ state shown in Fig. 16(a) (1.0 eV above E_F) are representative of the Al–Al_2O_3 interface states (S_1 and S_2 in Refs. 9 and 14) formed on this surface.

D. Surface core-level shifts

The Al($2p$) core level in the bulk oxide Al_2O_3 is observed to be chemically shifted 2.6 eV to greater binding energies than in bulk Al,[13] and is associated with charge transfer from the Al atom to the O atoms. Photoemission spectra for the sur-

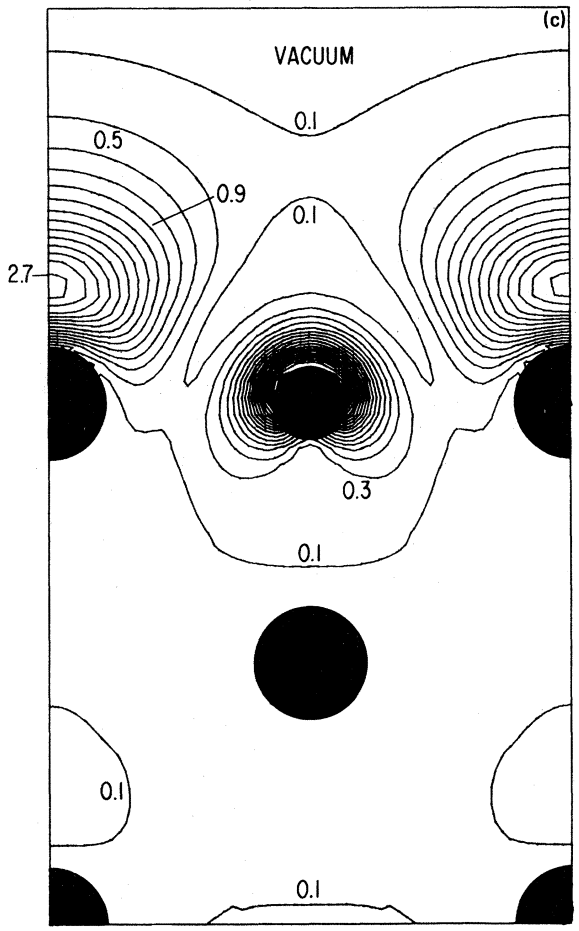

FIG. 16. *(Continued)*.

face Al(2*p*) level on the (111) surface shows a chemically shifted peak at 1.4 eV greater binding energy below about 100 L O exposure.[5] At higher exposures, a peak at 2.6 eV greater binding energy begins to grow, indicating the formation of the bulk oxide.

By contrast, for exposure less than about 100 L, the photoemission intensity from the (001) surface is nearly equally distributed in a region of up to 3 eV greater binding energies.[5,7] At higher exposure on the (100) surface, both the 1.4-eV peak and 2.7-eV peaks are present with about the same relative intensities.[7] This behavior has been interpreted in terms of an island growth oxidation model on the Al(001) surface.[1,8] In this model, an amorphous oxide film immediately forms on the (100) face upon exposure to oxygen followed by island growth. Adopting this model, the presence of the shoulder at 1.4 eV higher binding energy[7] indicates that a substantial number of the oxygen atoms are involved in some sort of intermediate bonding state. Our calculated results show a surface Al atom core-level shift of 1.5 eV to greater binding energy and no shift for any of the other Al atoms. This suggests that, in the initial stages of oxidation, a substantial number of the oxygen atoms are located in the fourfold hollow site as has been suggested by Eberhardt and Kunz[7] who interpreted their results as evidence for penetration of the O atoms into the Al substrate. As noted earlier, this is also in agreement with the dramatic decrease in calculated and observed work function on the (100) surface,[1,2] while little change in work function occurs for the (111) and (110) surfaces. Finally, as stated earlier, we find no surface core-level shift for the clean Al(001) nine-layer film in agreement with recent measurements.[31]

V. CONCLUSIONS

We have presented results of self-consistent calculations for a clean nine-layer Al(001) slab and for the same slab with a (1×1) monolayer of O atoms on each surface located in the fourfold hollow sites and coplanar with the surface Al atoms.

For the clean Al(001) slab, surface state-surface resonance bands were found which are in good agreement with angular resolved photoemission measurements and with our earlier non-self-consistent result.[28] Our theoretical work function value of 4.7 ± 0.1 eV, obtained using the Wigner interpolation formula[20,25] for exchange and correlation, is in good agreement with the Gepstad *et al.*[1] experimental value of (4.41 ± 0.03) eV. No surface core-level shift was found for the clean Al slab, in agreement with photoemission measurements[31] of the Al(2*p*) core level. Contrary to Ref. 31, however, we find no evidence of a broadening (possibly due to a crystal field effect at surface[31]) of the surface Al(2*p*) core level relative to a bulk level when the Al(2*p*) core levels are calculated as band states. As noted above, this may be due to the neglect, in the present calculation, of nonspherical contributions to the potential inside the muffin-tin spheres which could be especially critical in determining possible crystal field splitting in the case of a very localized state such as a core state.

For the Al(001)/O slab, the calculated reduction in the work function (0.6 eV) is in good agreement with the experimentally determined value of 0.5–0.8 eV (Ref. 1) for this surface. Spectroscopically, prominent O(2*p*) peaks on the surface-layer DOS at -8.0 and -10.0 eV below E_F are in good agreement with photoemission measurements.[5,7] Additional structures, at 1.0 and 1.8 eV above E_F, due to oxygen-induced surface reso-

nance states, were related to measured unoccupied interface states (S_1 and S_2 in Refs. 9 and 14) observed by surface soft-x-ray absorption spectroscopy. Detailed contour plots of the charge density for both the O($2p$) states and O-induced surface resonances were presented in order to reveal the nature of the chemical bond. The overall bonding with the surface Al atoms appears ionic in character with significant charge transfer onto the O atom, as expected, forming a quite localized surface structure, i.e., the effects due to the presence of the O atoms on the surface were found to be rapidly screened out on going in from the surface towards the bulk. Finally, a surface core-level shift of 1.5 eV to greater binding energy was found for the surface Al atom (and not for any of the other Al atoms). This value is in excellent agreement with the 1.4-eV Al($2p$) shift measured by Eberhardt and Kunz.[7] This indicates that, in the initial stages of oxidation, a substantial number of O atoms are chemisorbed into the fourfold hollow sites as has been suggested by Eberhardt and Kunz,[7] and a recent EXAPFS[12] measurement for the Al–O band length. It is also in agreement with results of a self-consistent cluster calculation by Messmer and Salahub[16] and is consistent with the dramatic decrease in observed and calculated work function.[1]

ACKNOWLEDGMENTS

This work was supported by the National Science Foundation (Grant No. DMR 77-23776), the U.S. Department of Energy, and the Swiss National Science Foundation.

---

*Present address: Physics Department, College of William and Mary, Williamsburg, VA 23185.

†Present address: EPFL–Laboratoire de Physique Appliquée, CH-1003 Lausanne, Switzerland.

[1] J. K. Grepstad, P. O. Gartland, and B. J. Slagsvold, Surf. Sci. 57, 348 (1976); P. O. Gartland, *ibid.* 62, 183 (1977).

[2] P. Hofmann, W. Wyrobisch, and A. M. Bradshaw, Surf. Sci. 80, 344 (1979).

[3] S. A. Flodström, R. Z. Bachrach, R. S. Bauer, and S. B. M. Hagström, Phys. Rev. Lett. 37, 1282 (1976).

[4] K. Y. Yu, J. N. Miller, P. Chye, W. F. Spicer, N. D. Lang, and A. R. Williams, Phys. Rev. B 14, 1446 (1976).

[5] R. Z. Bachrach, S. A. Flodström, R. S. Bauer, S. B. M. Hagström, and D. J. Chadi, J. Vac. Sci. Technol. 15, 488 (1978).

[6] S. A. Flodström, C. W. B. Martinsson, R. Z. Bachrach, S. B. M. Hagström, and R. S. Bauer, Phys. Rev. Lett. 40, 907 (1978).

[7] W. Eberhardt and C. Kunz, Surf. Sci. 75, 709 (1978).

[8] C. W. B. Martinson and S. A. Flodström, Surf. Sci. 80, 306 (1979).

[9] A. Bianconi, R. Z. Bachrach, S. B. M. Hagström, and S. A. Flodström, Phys. Rev. B 19, 2837 (1979).

[10] C. W. B. Martinson and S. A. Flodström, Solid State Commun. 30, 671 (1979).

[11] W. Eberhardt and F. J. Himpsel, Phys. Rev. Lett. 42, 1375 (1979).

[12] M. L. den Boer, T. L. Einstein, W. T. Elam, R. L. Park, and L. D. Roelofs, Phys. Rev. Lett. 44, 496 (1980). A surface extended x-ray-absorption fine structure (EXAFS) study for clean Al surfaces is given by A. Biancono and R. Z. Bachrach, Phys. Rev. Lett. 42, 104 (79). An EXAFS study for a sample of 100-L-oxygen Al(111) is given by L. I. Johansson and J. Stöhr, Phys. Rev. Lett. 43, 1882 (1979).

[13] A. Barrie, Chem. Phys. Lett. 19, 109 (1973).

[14] A. Bianconi, R. Z. Bachrach, and S. A. Flodström, Phys. Rev. B 19, 3879 (1979).

[15] N. D. Lang and A. R. Williams, Phys. Rev. Lett. 34, 531 (1975); Phys. Rev. B 18, 616 (1978). Also see Ref. 4.

[16] R. P. Messmer and D. R. Salahub, Phys. Rev. B 16, 3415 (1977); D. R. Salahub, M. Roche, and R. P. Messmer, *ibid.* 18, 6495 (1978); J. Harris and G. S Painter, Phys. Rev. Lett. 36, 151 (1976).

[17] G. S. Painter, Phys. Rev. B 17, 662 (1978).

[18] I. P. Batra and S. Ciraci, Phys. Rev. Lett. 38, 774 (1977).

[19] H. Krakauer, M. Posternak, and A. J. Freeman, Phys. Rev. B 19, 1706 (1979).

[20] M. Posternak, H. Krakauer, A. J. Freeman, and D. D. Koelling, Phys. Rev. B 21, 5601 (1980).

[21] D. D. Koelling, A. J. Freeman, and F. M. Mueller, Phys. Rev. B 1, 1318 (1970).

[22] P. Hohenberg and W. Kohn, Phys. Rev. 136, B864 (1964); W. Kohn and L. J. Sham, Phys. Rev. 140, A1133 (1965); 145, 561 (1966); N. D. Lang and W. Kohn, Phys. Rev. B 3, 1215 (1971).

[23] We use a semirelativistic formulation developed by D. D. Koelling and B. N. Harmon, J. Phys. C 10, 3107 (1977).

[24] S. L. Cunningham, Phys. Rev. B 10, 4988 (1974).

[25] For the corrected form of Wigner's original formula see D. Pines, *Elementary Excitations in Solids* (Benjamin, New York, 1963), Eq. (3.58).

[26] S. P. Singhal and J. Callaway, Phys. Rev. B 16, 1744 (1977).

[27] E. Caruthers, L. Kleinman, and G. Alldredge, Phys. Rev. B 8, 4570 (1973). These authors also calculated surface states for the Al(110) and Al(111) surfaces at high symmetry points of the 2D Brillouin zone: Phys. Rev. B 9, 3325 (1974); 9, 3330 (1974).

[28] H. Krakauer, M. Posternak, and A. J. Freeman, Phys. Rev. Lett. 41, 1072 (1978).

[29] P. O. Gartland and B. J. Slagsvold, Solid State Commun. 25, 489 (1978).

[30] G. V. Hansson and S. A. Flodström, Phys. Rev. B 18, 1562 (1978).

[31] W. Eberhardt, G. Kalkoffen, and C. Kunz, Solid State Commun. 32, 901 (1979).

[32] J. C. Slater, *Symmetry and Energy Bands in Crystals* (Dover, New York, 1972), see pp. 99 and 312.